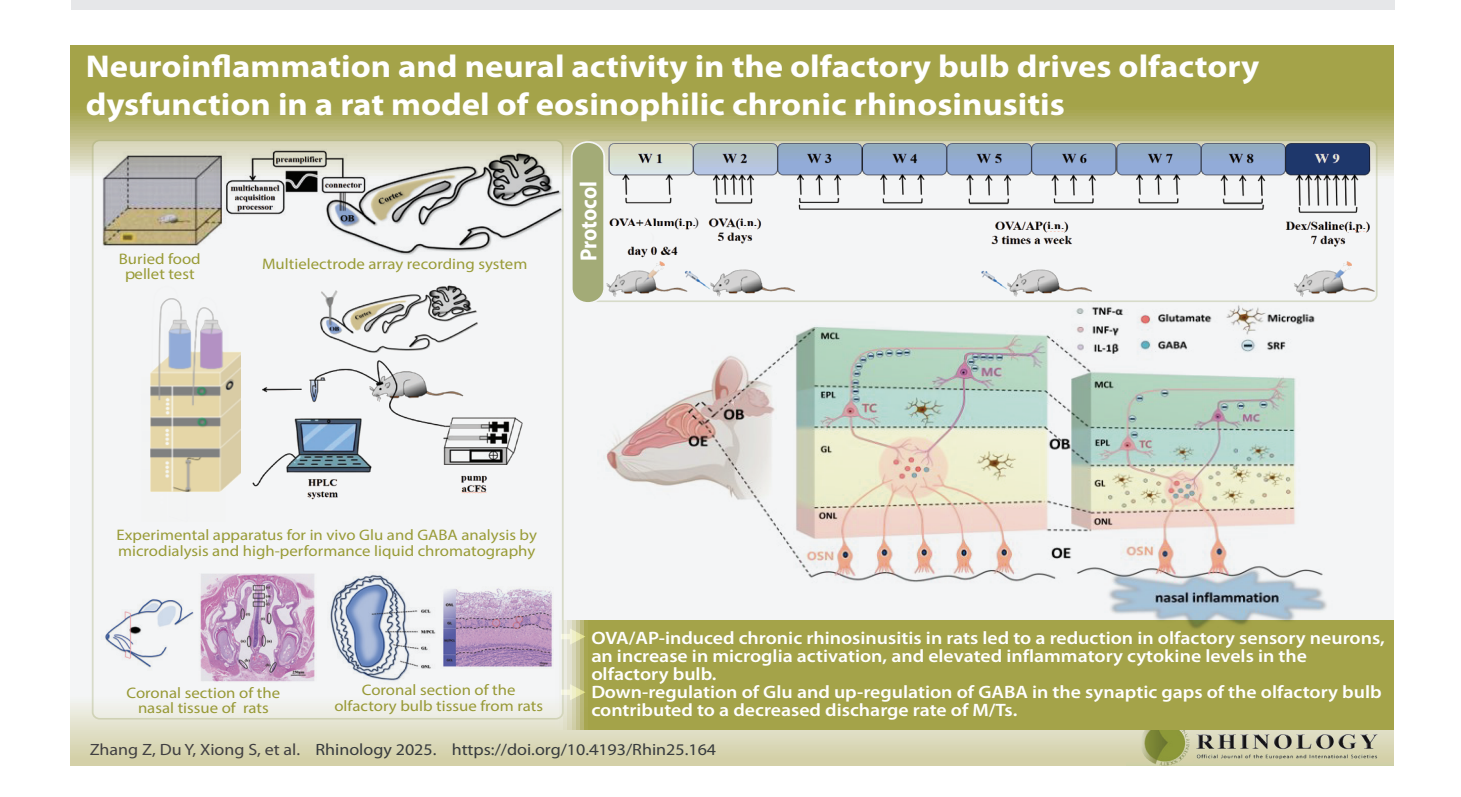
Neuroinflammation and neural activity in the olfactory bulb drives olfactory dysfunction in a rat model of eosinophilic chronic rhinosinusitis

Zhidi Zhang¹, Yali Du¹, Shan Xiong¹, Wanxin Cao², Hailing Jiang¹, Jiayue Wang¹, Mengqin Li¹, Ying Hu¹, Furong Ma^{1*}, Yinghong Zhang^{1*}

Rhinology 64: 1, 0 - 0, 2026 https://doi.org/10.4193/Rhin25.164



Abstract

Background: Chronic rhinosinusitis (CRS) is a common cause of olfactory dysfunction (OD), and eosinophilic CRS is one of the subtypes characterized by eosinophilic infiltration. Animal models of olfactory dysfunction in eosinophilic CRS are necessary for exploring potential therapeutic strategies. Glucocorticoids are therapeutic for eosinophilic CRS-OD and the mechanism of action requires further exploration. Methodology: The eosinophilic CRS-OD rat model was induced by intranasal administration of ovalbumin (OVA) and Aspergillus oryzae protease (AP) for 8 weeks, followed by intraperitoneal injection of dexamethasone. Olfactory function was assessed behaviorally, neuronal activity electrophysiologically, and neurotransmitter/inflammatory factor levels via high-performance liquid chromatography (HPLC). Histological analyses of nasal tissue and the olfactory bulb were performed. Results: All OVA/AP-induced eosinophilic CRS-OD rats developed chronic nasal inflammation and olfactory dysfunction. Reduced olfactory bulb (OB) volume was accompanied by thinning of the olfactory neuron layer (ONL) and the glomerular layer (GL). The OB exhibited increased microglia and elevated inflammatory cytokine expression. Further analysis revealed decreased glutamate (Glu), increased γ-aminobutyric acid (GABA), and a significant reduction in the spontaneous firing rate (SFR) of mitral/tufted cells (M/Ts) within the OB. Dexamethasone treatment significantly ameliorated olfactory impairment in this model, decreasing OB microglia numbers and inflammatory cytokine levels, and significantly increasing M/T SFR. Conclusions: Microglia-mediated neuroinflammation contributes to abnormal neural activity in the olfactory bulb, which may be one mechanism for the development of eosinophilic CRS-OD. The neuroprotective effect of dexamethasone, mediated through microglial inhibition, highlights microglia as an important therapeutic target for eosinophilic CRS-OD.

Key words: olfactory bulb, microglia, chronic rhinosinusitis, neural activity, dexamethasone

CRS-induced olfactory dysfunction and neuroinflammation

Introduction

The nasal cavity is in prolonged contact with various airborne allergens, triggering an immune-inflammatory response that often leads to chronic nasal inflammatory diseases such as chronic rhinosinusitis (CRS) (1). Olfactory dysfunction (OD) significantly impacts patient quality of life, and CRS is a major cause of OD, affecting up to 80% of CRS patients (CRS-OD) (2). Eosinophilic CRS is one of the subtypes characterized by eosinophilic infiltration. Previous studies have suggested that hyposmia occurs in chronic sinusitis because nasal obstruction factors prevent odors from reaching the olfactory epithelium. Recently, a significant reduction of olfactory sensory neurons (OSN) in the olfactory epithelium was observed using an animal model of eosinophilic CRS-OD induced by ovalbumin (OVA) and Aspergillus oryzae protease (AP) $^{(3)}$. Further suggests that olfactory impairment may be the result of direct damage to the olfactory epithelium, particularly OSN (4).

Although some studies have addressed OSN reduction, OSNs project directly from the olfactory epithelium to the olfactory bulb (OB). The role of the OB in CRS-OD pathogenesis, however, remains poorly investigated. Functional magnetic resonance imaging studies reveal reduced olfactory bulb volume in CRS patients with OD ⁽⁵⁾. Furthermore, increased microglial activation and neuroinflammatory cytokine expression are observed in the OB of patients with Alzheimer's disease, Parkinson's disease, or other neurodegenerative disorders featuring OD ^(6,7). Intranasal lipopolysaccharide (LPS) administration in mice also induces olfactory deficits and increases the number of OB microglia ^(8,9). Collectively, these findings suggest microglia-mediated neuroinflammation contributes significantly to OD, but its specific mechanism in CRS-OD is unclear.

Glucocorticoids are first-line therapy for CRS-related olfactory impairment ⁽¹⁰⁾. Dexamethasone exerts potent anti-inflammatory effects and significantly inhibits microglial activation via the glucocorticoid receptor ⁽¹¹⁾. As the relay station of the olfactory pathway, the OB is crucial for olfactory signal processing, yet its structure and internal neural circuitry are highly complex. Therefore, this study investigated neuroinflammation and neural activity within the OB in a rat model of OVA/AP-induced CRS, along with the effects of dexamethasone intervention.

Materials and methods

Animals

Healthy 4-week-old Sprague-Dawley rats (n=46) were housed under standard conditions (12h light/dark cycle, 22±1°C, 50-60% humidity) with ad libitum access to food/water. All procedures were approved by the Animal Ethics Committee of Peking University (No. A2024063).

Experimental protocol

Experimental rats were randomly divided into 4 groups, refer to

Kim et al. (12) modeling method see Figure 1A. CRS-OD was induced in SD rats by intranasal OVA/AP administration for 8 weeks, as previously described. Intraperitoneal (i.p.) injection provides >90% bioavailability for dexamethasone, like intravenous (i.v.) administration due to rapid peritoneal absorption and avoidance of first-pass metabolism (13). Dexamethasone (Dex) or saline was intraperitoneally injected for 7 days (Supplementary Method 1).

To avoid the potential risk of death and discomfort caused by anesthesia, intranasal administration was done without anesthesia. Ensure that the rat is awake and head up when dropping to avoid acute lung injury due to aspiration. The solution was dropped into the anterior nostrils of the rats in small amounts using a pipette gun to ensure complete absorption. The rats in the control and experimental groups were euthanized at the end of the 8th week, and the rats in the saline and dexamethasone groups were euthanized at the end of the 9th week. Nasal tissues, blood and nasal lavage fluid of rats were collected for analysis.

Olfactory behavior test (BFT)

The buried food test is a classic behavioral method for testing the olfactory function of animals (14) (Figure 1B and Supplementary Method 2). The time points at which the ball-burying experiment was conducted were at week 0, week 6, week 8, and week 9.

Electrophysiology measurement

All animals were anesthetized using isoflurane (anesthesia induction: 3-5% for 3 minutes; anesthesia maintenance: 1-2%; flow rate 0.2–0.3L/min) and placed in a stereotaxic head frame on a heating blanket. A craniotomy was performed over the right OB (anteroposterior = 6.6 mm, mediolateral = 1.0 mm, dorsoventral = 4.5 mm), conforming to rat brain stereotaxic coordinates (15). Two stainless steel screws were anchored to the skull and wrapped with a reference wire. Using tweezers, the dura mater was carefully removed under a surgical microscope to expose the OB tissue. Then a 16-channel silicon electrode (4×4 array, the Chinese Academy of Sciences, Beijing, China) was advanced into the OB along the dorsal-ventral axis for singleunit recording of mitral/tufted cells (M/Ts). The output of the 16-channel silicon electrode was connected to a 16-channel preamp amplifier (Plexon, Inc., TX, USA) to record the data of the spontaneous firing rate (SFR). The analyses were conducted using Offline Sorter software, version 4.2.0 (Plexon, Dallas, TX, USA) and Neuroexplorer software, version 5 (Nex Technologies, Littleton, MA, USA), as previously described (16) (Figure 1C).

HPLC system for glutamate and γ-aminobutyric acidA steel catheter (15 mm, CMA, Solan, Sweden) was placed in the

right OB and fixed to the skull with cranial screws and dental cement. A 2-mm microdialysis probe (CMA, Solan, Sweden) was

Zhang et al.

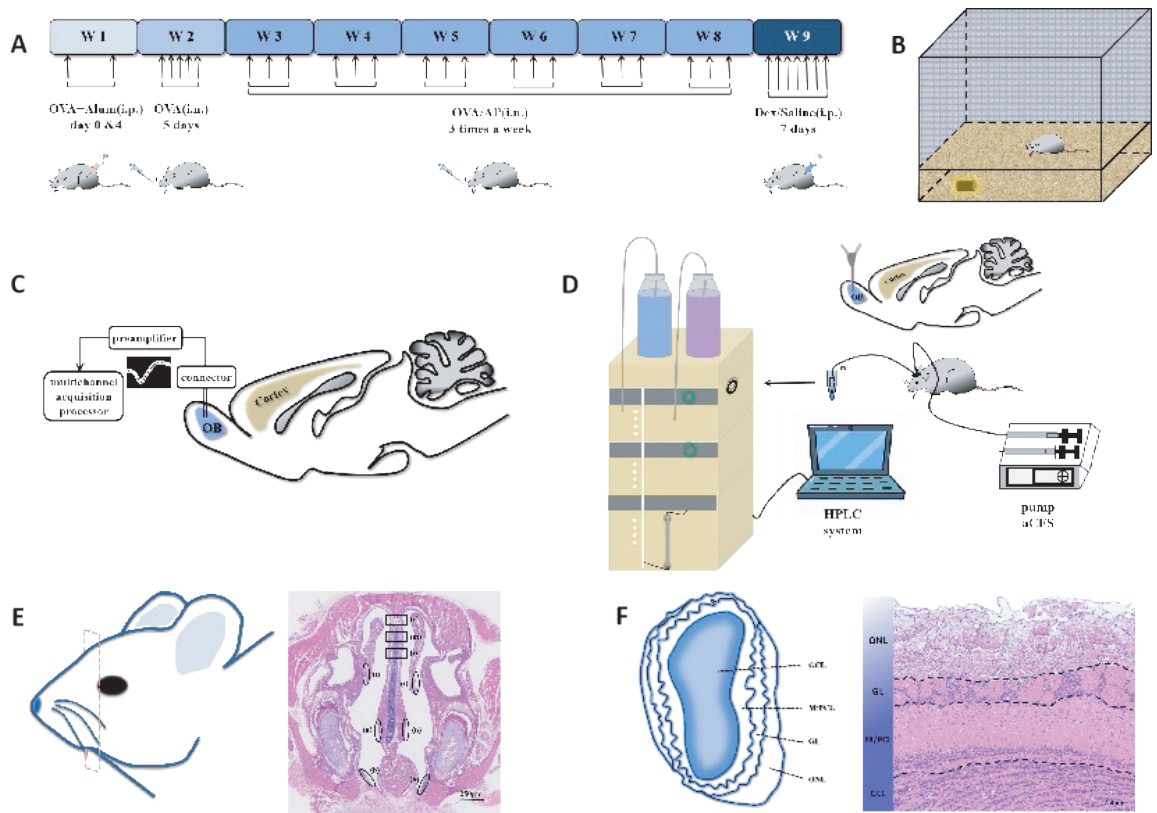


Figure 1. Experimental methods. (A) Protocol for CRS-OD rat model induction and intranasal treatments. OVA, ovalbumin; Alum, aluminum hydroxide solution; AP, Aspergillus oryzae protease; i.p. intraperitoneal; i.n. intranasal. (B) Schematic of the buried food-pellet test in rat. (C) Schematic diagram of the multielectrode array recording system. (D) Schematic diagram of the experimental apparatus for in vivo Glu and GABA acid analysis by micro-dialysis and high-performance liquid chromatography (HPLC). (E) Section selected for epithelial thickness assessment is positioned immediately anterior to anterior border of eyes in SD rat. Olfactory areas for measurement are (s) superior, (m) middle, and (i) inferior nasal septum; respiratory areas are (t) turbinate, (n) nasal septum, and (b) basis nasi (scale bar 250 µm). (F) Schematic diagram showing OB layers in a coronal section. The structure of each layer of the olfactory bulb is as follows: olfactory neuron layer (ONL), glomerular layer (GL), mitral cell and plexiform cell layer(M/PCL), and granular cell layer (GCL).

inserted into the guide tube and the artificial cerebrospinal fluid was instilled at a rate of 2 $\mu L/min$. Samples were collected every 30 min. A high-performance liquid chromatography (HPLC) system (Shimadzu Corporation, Kyoto, Japan) was used for all dialysate samples to detect glutamate (Glu) and γ - aminobutyric acid (GABA). The chromatographic separation was carried out on the Shimadzu C18 column (150 \times 4.6 mm, 5 mm particle size) using a mobile phase composed of a mixture of methanol-phosphate buffer (0.02 mol/L, pH = 6.8; 20:80, v/v) filtered through a 0.45 mm nylon filter and degassed under ultrasound for 30 min. The flow rate of the system was 1.0 mL/min (Figure 1D).

Histological analysis

Rats were euthanized via urethane anesthesia (20%, 7ml/kg) and perfused. Nasal tissues and OB were fixed in 4% paraformaldehyde. Nasal specimens were decalcified (10% EDTA, 14 days), paraffin-embedded, and coronally sectioned (4 μ m) anterior to the ocular edge. OB tissues were sectioned sagittally. Sections of olfactory bulb tissue and nasal tissue were dehydra-

ted in paraffin sections. The sections were stained with hematoxylin and eosin (HE), and inflammatory lesions, including eosinophil infiltration counts, epithelial thickness, and subepithelial thickness, were measured in three respiratory epithelial regions and three olfactory epithelial regions on each side of the left and right nasal cavity (Figure 1E), and the results were calculated and averaged. To quantify the effect of OVA/AP on the OB layer, we selected a slice from the middle of the OB and measured the area of each layer: olfactory neuron layer (ONL), glomerular layer (GL), mitral cell and plexiform cell layer (M/PCL) and granular cell layer (GCL) (Figure 1F).

Olfactory sensory neurons were in the olfactory epithelium and were identified by staining using olfactory marker protein (OMP, ab183947-10, Abcam) (Supplementary Method 3). The number of OMP-positive cells in the right and left regions of the nasal septum was calculated using ImageJ software, and the results were averaged. The level of OMP expression in olfactory bulb tissue was assessed according to the average optical density (AOD), and five 200× fields of view were selected from the secti-

CRS-induced olfactory dysfunction and neuroinflammation

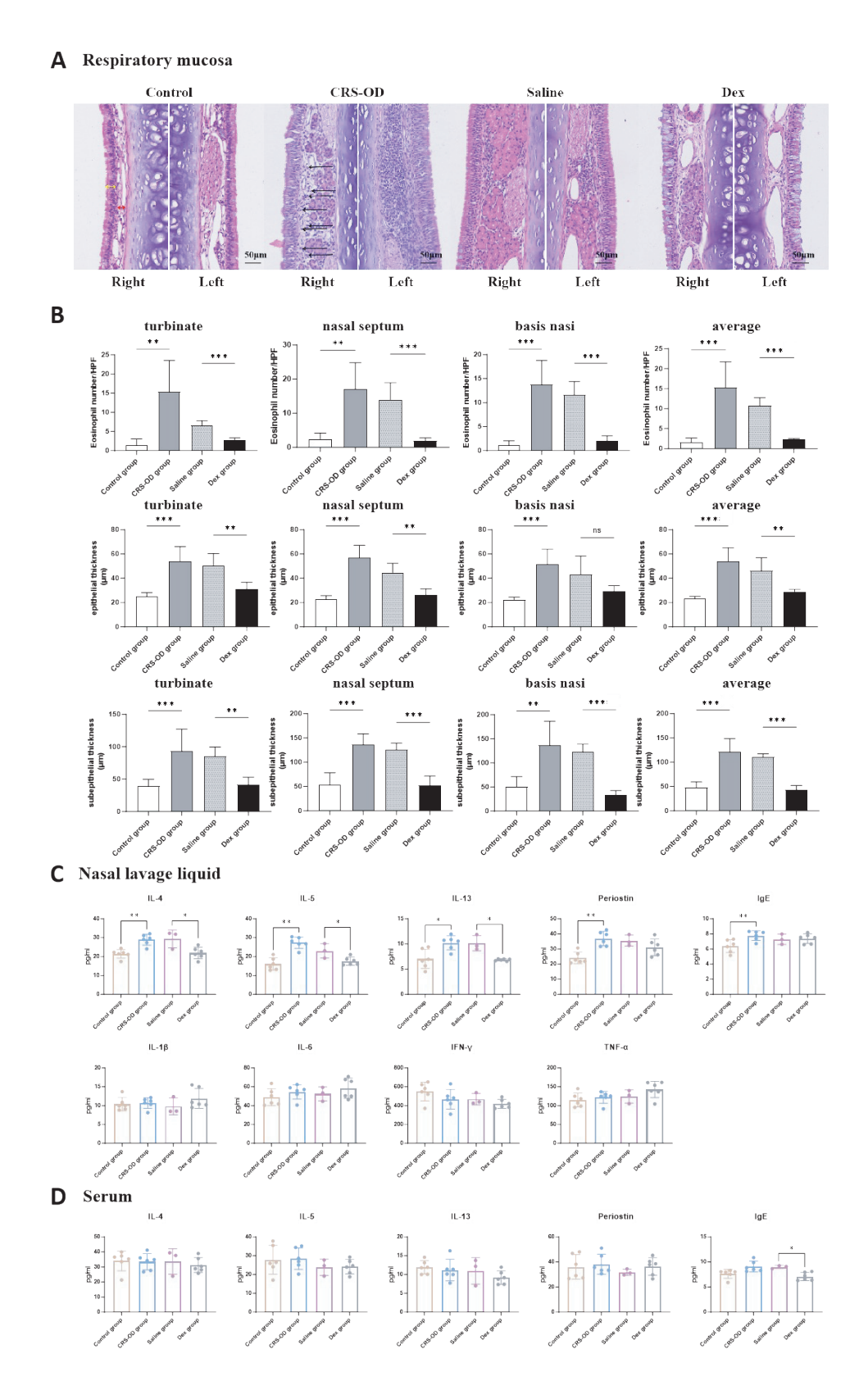


Figure 2. OVA/AP administration induced chronic rhinosinusitis. (A) H&E staining of mucous membranes (scale bar 50µm) in the respiratory zone in Control (n=6), CRS-OD (n=6), Saline (n=3), and Dex groups (n=6). Black arrows represent eosinophils. Yellow arrows represent epithelial thickness. Red arrows represent subepithelial thickness. (B) Quantitation of eosinophils, epithelial thickness and subepithelial thickness in respiratory areas. (C) Comparison of inflammatory cytokines in nasal lavage liquid from Control (n=6), CRS-OD (n=6), Saline (n=3), and Dex groups (n=6). (D) Comparison of inflammatory cytokines in serum from Control(n=6), CRS-OD (n=6), Saline (n=3), and Dex groups (n=6). ns, no significance. *P < 0.05. **P < 0.01. ***P < 0.001.

Zhang et al.

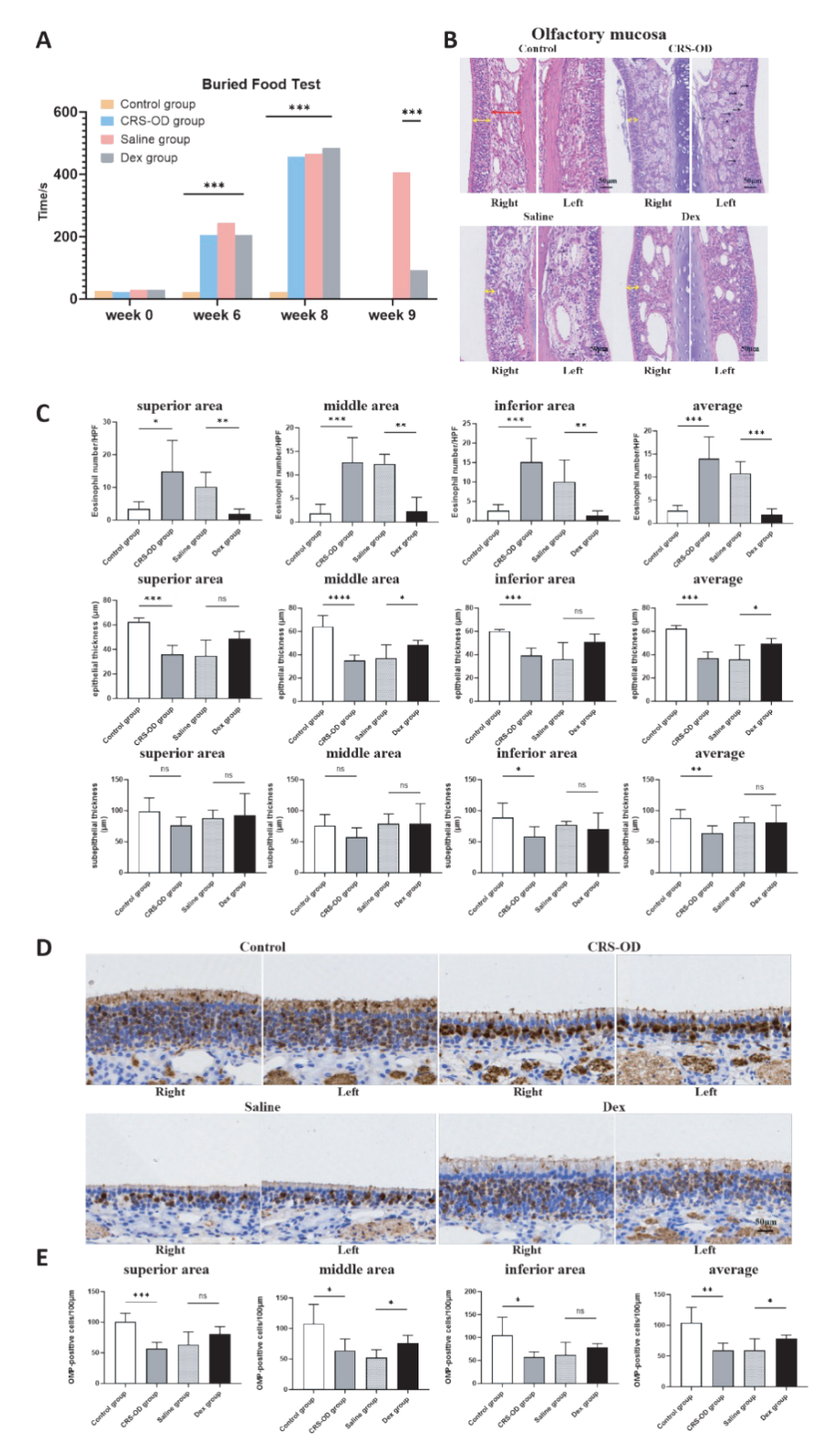


Figure 3. OVA/AP administration impairs olfactory function and olfactory sensory neurons. (A) The buried food test showed impairment of olfactory function after OVA/AP administration and improvement of olfactory function after dexamethasone treatment. Control group: n=12, CRS-OD group: n=12, Saline group: n=10, Dex group: n=12. (B) H&E staining of mucous membranes in the olfactory zone in Control, CRS-OD, Saline, and Dex groups (scale bar 50µm). Black arrows represent eosinophils. Yellow arrows represent epithelial thickness. Red arrows represent subepithelial thickness. (C) Quantitation of eosinophils, epithelial thickness and subepithelial thickness in olfactory areas. Control group: n=6, CRS-OD group: n=6, Saline group: n=3, Dex group: n=6. (D) Representative photomicrographs of immunohistochemistry with the anti-OMP antibody of olfactory mucosa to detect mature olfactory sensory neurons in Control, CRS-OD, Saline, and Dex groups (scale bar 50µm). (E) Quantitation of OMP-positive cells of the olfactory epithelium. Control group: n=6, CRS-OD group: n=6, Saline group: n=3, Dex group: n=6. Ns, no significance. *P < 0.05. **P < 0.01. ***P < 0.001.

CRS-induced olfactory dysfunction and neuroinflammation

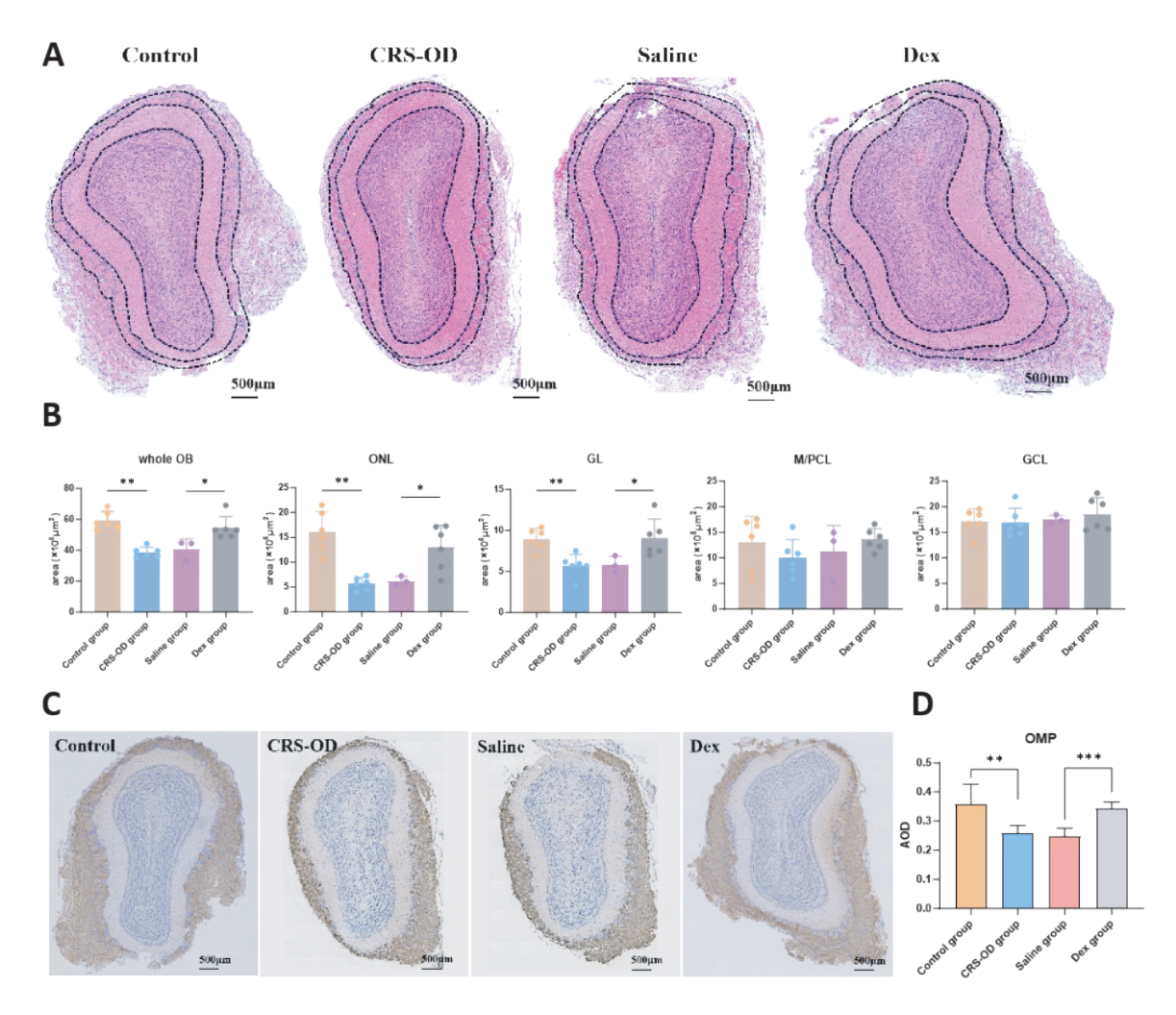


Figure 4. OVA/AP administration impairs ONL and GL in the olfactory bulb. (A) Graphs showing areas of whole OB, ONL, GL, EPL, M/PCL, and GCL. H&E staining of OB in Control (n=6), CRS-OD (n=6), Saline (n=3), and Dex groups (n=6) (scale bar $500\mu m$). (B) The volume of the olfactory bulb and the area of each layer were compared in the Control, CRS-OD, Saline, and Dex groups. (C) Immunostaining sections showed OMP expression in the olfactory bulb. (D) Quantification of OMP in Control (n=6), CRS-OD (n=6), Saline (n=3), and Dex groups (n=6). *P < 0.05. **P < 0.01. ***P < 0.001.

ons, and the results were calculated and averaged. To evaluate the ratio of lba1+ cells (microglia), immunofluorescence staining was performed (Supplementary Method 4). ImageJ software was used to evaluate the expression of microglia according to the mean gray value. Five 200-fold fields were selected from the sections, and the calculated results were averaged.

Nasal lavage fluid and OB tissue cytokine analysis

Nasal lavage fluid was collected via pharyngeal PBS infusion and anterior nostril aspiration. Olfactory bulb (OB) tissues were homogenized in PBS, centrifuged (12,000×g, 10min), and supernatants analyzed for Th1/Th2/Th17 cytokines (IL-4, IL-5, IL-13, IgE,

periostin, IL-1 β , IL-6, IFN- γ , TNF- α) using ELISA kits (Dogesce).

Statistical analysis

Data values were expressed in mean and standard deviation. The Mann-Whitney U test was used to assess differences between the 2 groups. A P-value threshold of <0.05 was used to indicate statistical significance. Statistical analyses were performed using SPSS (Version 26, SPSS Inc., Chicago, IL, USA).

Results

OVA/AP administration-induced chronic rhinosinusitisChronic nasal inflammation severity was assessed by inflammatory cell infiltration, epithelial thickness, and subepithelial

Rhinology Vol 64, No 1, February 2026

Zhang et al.

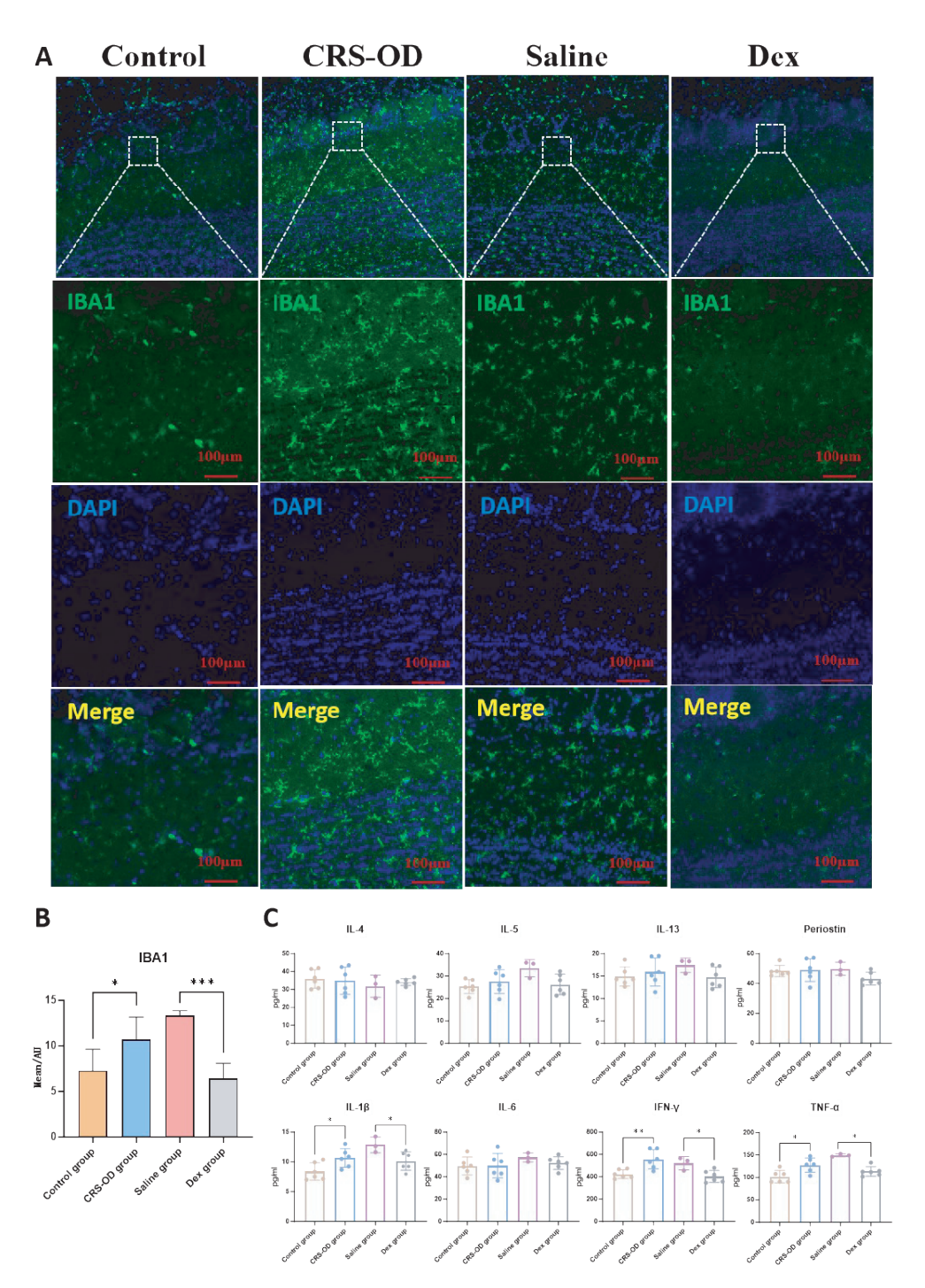


Figure 5. OVA/AP induces increased microglia and inflammatory cytokines in the olfactory bulb. (A) Immunostained sections, showing IBA1-positive cells in Control, CRS-OD, Saline, and Dex groups (scale bar $100\mu m$). (B) Quantitative expression of IBA1-positive cells in Control (n=6), CRS-OD (n=6), Saline (n=3), and Dex groups (n=6). (C) The expression levels of inflammatory cytokines in Control (n=6), CRS-OD (n=6), Saline (n=3), and Dex groups (n=6). *P < 0.05. **P < 0.01. ***P < 0.001.

thickness. Eosinophil counts in the respiratory mucosa, along with epithelial and subepithelial thicknesses, were significantly increased in the CRS-OD group versus controls (Figure 2A, B). In addition, the expression of inflammatory cytokines in nasal lavage fluid is another indicator for assessing the inflammatory state of the nasal cavity. Inflammatory cytokines IL-4, IL-5, IL-13,

periostin, and IgE showed significantly elevated levels in nasal lavage fluid in the CRS-OD group (Figure 2C). In contrast, serum IgE levels were decreased (Figure 2D). Dexamethasone treatment significantly reduced respiratory mucosal eosinophils and NLF inflammatory cytokine levels (Figure 2).

CRS-induced olfactory dysfunction and neuroinflammation

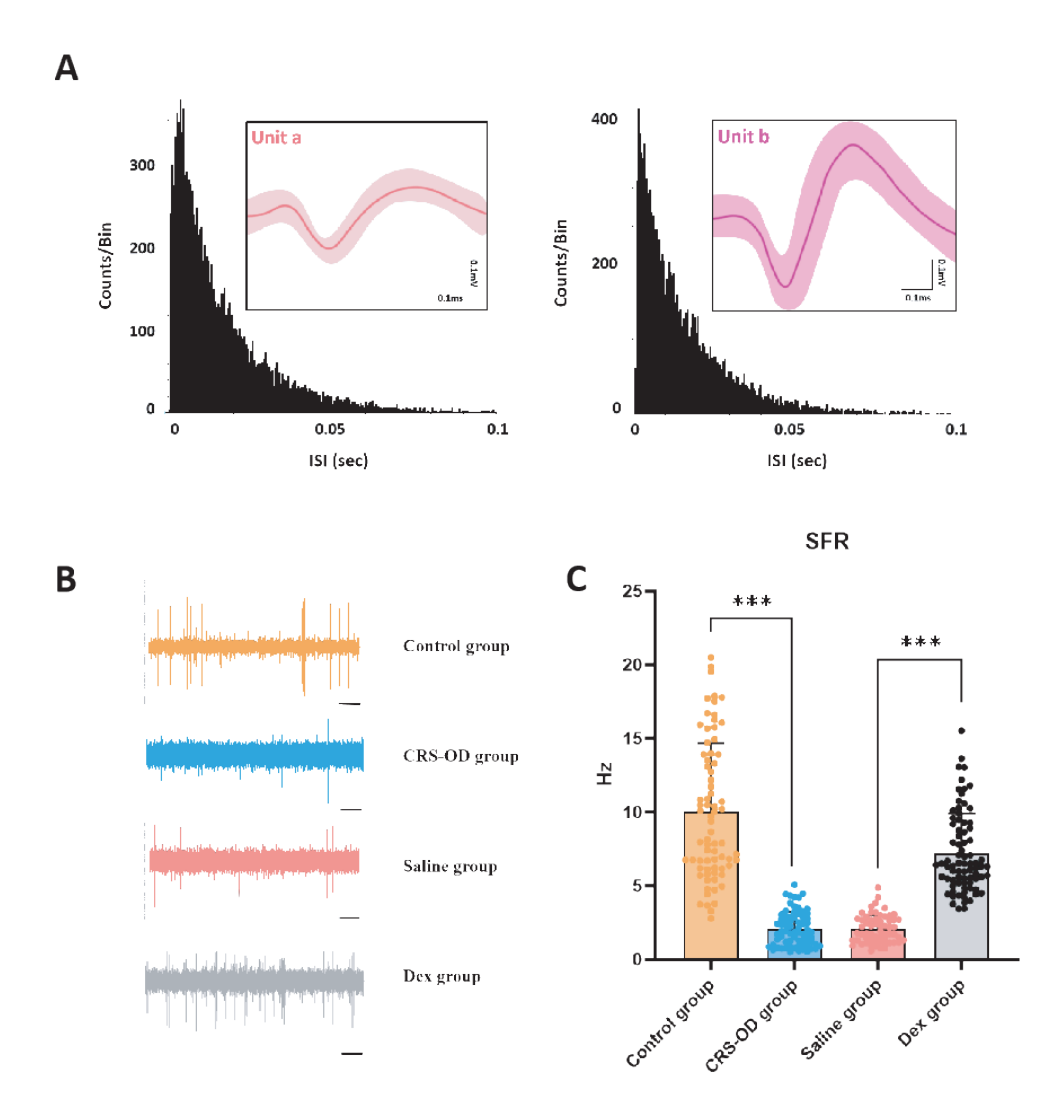


Figure 6. OVA/AP administration reduces SFR of M/Ts in the olfactory bulb. (A) Typical two units (unit a; unit b) of 800-µs average waveforms and burst firing pattern observed in the interspike interval histogram (ISI) of a typical neuron recorded from the silicon electrode in the olfactory bulb. Scales: 0.1mV; 0.1 ms. (B) Example of spike discharges recorded from the gold-based microelectrode arrays in Control (n=6), CRS-OD (n=6), Saline (n=3), and Dex groups (n=6). Scales: 2 s. (C) Summary graphs of SFR of neurons in Control (n=6), CRS-OD (n=6), Saline (n=3), and Dex groups (n=6). ***P < 0.001.

OVA/AP administration impairs olfactory function and OSN Olfactory function, assessed by the buried food test at baseline (week 0), week 6, and week 8, was impaired in CRS-OD rats, which exhibited significantly prolonged food-finding latency versus controls (Figure 3A). Within the olfactory mucosa, eosinophil counts were elevated, whereas epithelial and subepithelial thicknesses were significantly reduced in the CRS-OD group (Figure 3B, C). The number of OMP-positive cells (mature OSNs) was significantly decreased in the CRS-OD group olfactory epithelium (Figure 3D, E). Dexamethasone treatment significantly shortened food-finding latency and increased OSN numbers (Figure 3).

OVA/AP administration impairs ONL and GL in the OBOB volume was significantly reduced in the CRS-OD group versus controls, accompanied by thinning of the ONL and GL;

the mitral cell layer (MCL) and external plexiform layer (EPL) thicknesses remained unchanged (Figure 4A, B). OMP expression within the OB was also significantly reduced following OVA/AP administration (Figure 4C, D). Dexamethasone treatment significantly restored OB volume, ONL and GL areas, and OMP expression (Figure 4).

OVA/AP induces increased microglia and inflammatory cytokines in the OB

Iba1 immunofluorescence revealed significantly increased microglial density in the OB of CRS-OD rats compared to controls (Figure 5A, B). Levels of inflammatory cytokines (IL-1 β , IFN- γ , TNF- α) in OB homogenates were also significantly elevated in the CRS-OD group (Figure 5C). Dexamethasone treatment significantly reduced microglia, IL-1 β , IFN- γ , and TNF- α expression (Figure 5).

Zhang et al.

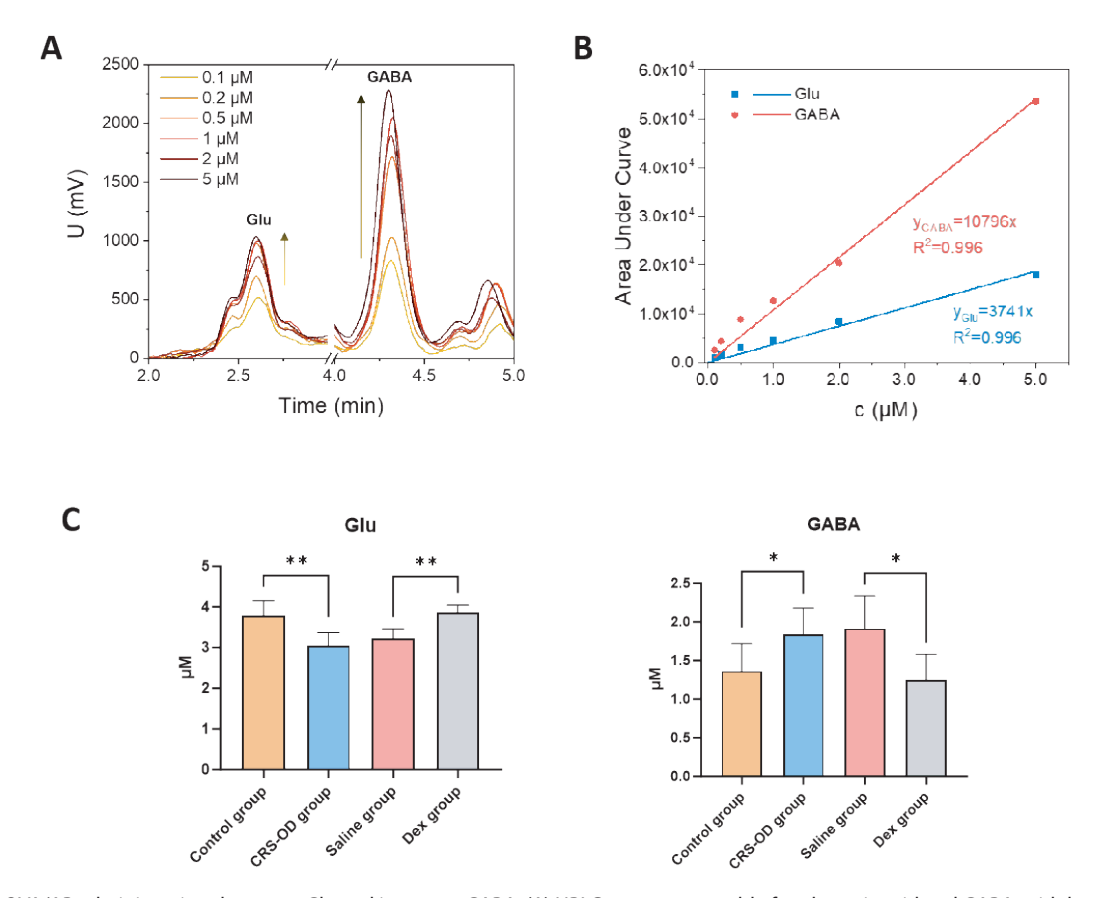


Figure 7. OVA/AP administration decreases Glu and increases GABA. (A) HPLC system was stable for glutamic acid and GABA acid detection. (B) HPLC system shows a good linear response toward Glu and GABA standard solution from 0.1 μ M to 5 μ M. (C) The expression of glutamic acid and GABA of the olfactory bulb in Control (n=6), CRS-OD (n=6), Saline (n=3), and Dex groups (n=6) was detected by the HPLC system. Glu, Glutamate; GABA, γ -aminobutyric acid. *P < 0.05. **P < 0.01.

OVA/AP administration reduces the SFR of M/Ts in the OB Analysis of individual neuron firing rates showed a significantly reduced spontaneous firing rate (SFR) of M/Ts in the CRS-OD group versus controls. Dexamethasone treatment significantly increased neuronal SFR (Figure 6).

OVA/AP administration decreases glutamate and increases GABA

HPLC calibration demonstrated good linearity for Glu and GABA standards (0.1-5 μ M; Glu: U(V) = 3741x, R² = 0.996; GABA: U(V) = 10796x, R² = 0.996) (Figure 7A, B). OB Glu levels were significantly decreased in the CRS-OD group versus controls but elevated after dexamethasone treatment. Conversely, OB GABA levels were significantly increased in the CRS-OD group and reduced by dexamethasone treatment (Figure 7C).

Discussion

To our knowledge, this is the first study demonstrating that peripheral OSN damage and OB microglial activation cause decreased synaptic Glu and increased GABA, directly reducing M/Ts excitability and olfactory signaling. Furthermore, dexamet-

hasone exerted neuroprotective effects within the OB, effectively reversing OVA/AP-induced olfactory impairment in this CRS model.

In the olfactory system, peripheral OSNs within the nasal olfactory mucosa receive odorants and project axons to the OB (17). These exposed neurons are highly vulnerable to environmental toxins and inflammatory stimuli. Intranasal OVA/AP administration effectively induced CRS. Kim et al. (12) established a mouse CRS model characterized by nasal mucosal thickening and inflammatory cell infiltration following intranasal OVA/AP. Rouyar et al. (18) also observed increased olfactory mucosal eosinophils following intranasal house dust mite (HDM) and Staphylococcus aureus enterotoxin B (SEB). Our study successfully established a rat model of eosinophilic CRS following intranasal OVA/AP administration. This was marked by significant thickening of the nasal mucosa, inflammatory cell infiltration, and elevated expression of inflammatory factors. Moreover, the olfactory mucosa showed significant eosinophil infiltration, accompanied by a notable reduction in olfactory sensory neurons. The substantial decrease in olfactory function observed in rats after OVA/ AP administration, as assessed by the buried ball test, suggests

CRS-induced olfactory dysfunction and neuroinflammation

that OVA/AP-induced chronic rhinosinusitis not only damages the nasal mucosa but also impairs olfactory function, severely affecting olfactory sensory neurons.

The olfactory bulb serves as the relay station for the olfactory pathway. OSN axons extend into the OB, where olfactory signals are integrated within glomeruli before being transmitted via M/ Ts to higher brain regions (17). However, studies examining the effects of intranasally induced nasal inflammation on the olfactory bulb are limited. In our study, OVA/AP-induced chronic rhinosinusitis in rats resulted in a significant reduction in olfactory bulb volume, with predominant reductions in the ONL and GL. Olfactory sensory neurons showed a similar reduction in expression as the olfactory epithelium. Furthermore, we found that neuroinflammation plays a significant role in the olfactory bulb's response to chronic rhinosinusitis. The number of microglia was increased, and the expression of key pro-inflammatory cytokines, including IL-1β, IFN-γ, and TNF-α, was elevated. Microglia, as immune cells of the central nervous system, are primarily responsible for recognizing and removing necrotic cells and pathogens. They are also involved in critical neural activities such as synaptogenesis, neurogenesis, and the release of neurotrophic factors under normal conditions. However, when neuronal injury and disturbances in microenvironmental homeostasis occur, microglia become activated, releasing pro-inflammatory cytokines like IL-1 β , IL-6, TNF- α , and IFN- γ , which inhibit neurogenesis and neuronal repair (19). Previous studies have demonstrated that intranasal LPS administration induces a significant reduction in olfactory bulb volume and elevated inflammatory cytokine levels, such as TNF- α and IFN- γ , in the olfactory bulb of mice with chronic rhinosinusitis (9, 20). In a mouse model of Toll-like receptor 3-induced upper respiratory inflammation, decreased OSNs in the olfactory epithelium, increased microglia in the olfactory bulb, and elevated levels of IL-1 β , IL-6, TNF- α , and IFN- γ were observed, suggesting that olfactory bulb neuroinflammation plays a central role in impairing olfactory function during nasal inflammation (21). Therefore, we speculate that chronic rhinosinusitis after prolonged nasal OVA/AP administration damages olfactory sensory neurons, and axonal fragmentation of olfactory sensory neurons activates microglia in the olfactory bulb to induce neuroinflammation, which in turn destroys nerve cells in the olfactory bulb.

The olfactory bulb contains various types of neurons, including mitral cells, tufted cells, granule cells, and OSNs. OSNs form synaptic connections with mitral and tufted cells (also referred to as plexiform cells), which release Glu as an excitatory neurotransmitter into the synaptic gap. These neurons are also influenced by the inhibitory neurotransmitter GABA (22). To further explore the impact of neuroinflammation on the olfactory bulb, we examined the spontaneous firing rate of individual neurons in the olfactory bulb of living rats. In OVA/AP-induced chronic rhinosinusitis in rats, we observed a significant reduction in the

spontaneous firing rate of olfactory bulb neurons compared to controls. Previous studies have reported similar reductions in neuronal activity, such as in models where zinc sulfate-induced nasal epithelial damage led to olfactory loss and decreased spontaneous neuronal firing in the olfactory bulb (23). Chronic hypoxia, too, has been shown to induce apoptosis in olfactory sensory neurons (24), and olfactory deficits in chronic intermittent hypoxia models have been linked to altered spontaneous activity in the olfactory bulb, including reductions in β - and γ-wave frequencies (25). In older mice with olfactory bulb injury, diminished excitatory postsynaptic potentials and reduced peak potentials were noted, suggesting a decline in neural activity within the olfactory bulb (26). Thus, the reduced electrical activity in olfactory bulb neurons may be directly associated with the destruction of olfactory sensory neurons. Although spontaneous firing reflects baseline excitability, stimulus-specific responses will be prioritized in future work to directly link neuroinflammation to coding deficits.

Looking further at the two neurotransmitters important in the olfactory bulb: Glu and GABA acid, the reduced levels of Glu in the synaptic gap may be related to the subsequent decrease in the number of olfactory sensory neurons, which further reduces the excitation of the M/Ts. Conversely, there is an increase in GABA in the olfactory bulb. GABA is mostly released by intermediate neurons such as granule cells and parabasal cells in the olfactory bulb, inhibiting nerve signaling. Additionally, the impact of microglia-mediated neuroinflammation on the neural circuits of the olfactory bulb cannot be overlooked. Microglia, when activated by pathogens or debris from damaged cells, release a large array of pro-inflammatory cytokines, including IL-1 β , TNF- α , and IL-6 (27). These inflammatory mediators can lead to synaptic dysfunction, blood-brain barrier disruption, and impaired Glu transport (28). In our study, intranasal administration of OVA/AP to rats caused the destruction of olfactory sensory neurons, activated microglia in the olfactory bulb, and triggered a neuroinflammatory response. This neuroinflammation further damaged neuronal synapses, disrupted neurotransmitter signaling, and ultimately reduced olfactory signaling.

Glucocorticoids are an effective drug for targeting inflammation (29). Not only does it reduce chronic rhinosinusitis, it has also been shown to be used in the treatment of neuroinflammatory conditions (30). Clinically dexamethasone is the first line of medication used to treat patients with CRS and is effective in reducing inflammation such as eosinophils and neutrophils in the nasal mucosa (29). Our study showed that dexamethasone reduced nasal inflammatory cells and inflammatory factors in a rat model of OVA/AP-induced chronic rhinosinusitis and protected the nasal mucosa and olfactory mucosa to restore normal function. In addition, the protective effect of dexamethasone in suppressing neuroinflammation is not negligible in many neurological disorders. Neuroinflammation induced by astrocyte

Zhang et al.

and microglia activation in acute fine meningitis was found (30). In traumatic brain injury, dexamethasone protects brain tissue by inhibiting hippocampal microglia activation, decreasing IL-1 expression, and reducing oxidative stress (31). Our study showed that dexamethasone effectively restored neurogenic olfactory impairment by reducing peripheral inflammation-induced neuroinflammation. We observed significant recovery of OB volume within 7 days of dexamethasone treatment, likely due to rapid suppression of microglia-mediated inflammation and neurotrophic effects. Dexamethasone reduces microglia and neuroinflammatory factors in the olfactory bulb, which reduces further neuroinflammatory damage to olfactory sensory neurons, M/Ts, and protects normal neuronal activity in the olfactory bulb. Microglia have important glucocorticoid receptors that bind to dexamethasone and inhibit microglia activation (11, 32). However, it has been found that LPS-induced neuroinflammation did not result in a reduction in microglia activation after 24 hours of dexamethasone administration, regardless of the route of administration (intranasal or intravenous) (33). Considering the importance of the dose at the time of administration, we used dexamethasone systemically for 7 consecutive days, and a reduction in microglia activation was observed, suggesting that short-term continuous dexamethasone is effective in suppressing neuroinflammation.

There are obvious limitations of this study. Although we focused on OVA/AP-mediated chronic rhinosinusitis, true chronic rhinosinusitis can induce a variety of responses leading to olfactory impairment. Our future work will also explicitly compare olfactory bulb neurotransmitter profiles in non-sinusitis olfactory disorder models (e.g., post-viral, traumatic, or age-related OD). While BFT is a validated olfactory screening tool, its susceptibility to motivational confounders is noted. Future studies will incorporate odorant-evoked local field potentials for direct functional correlation. In addition, the olfactory conduction pathway is extremely complex, and only pathophysiological changes in the primary olfactory structures (olfactory epithelium and olfactory

bulb) were observed in this study; as for the functional changes in the higher centers of olfaction, they are not clear and need to be further explained.

Conclusion

In this study, we demonstrated that OVA/AP-induced chronic rhinosinusitis in rats led to a reduction in olfactory sensory neurons, an increase in microglia activation, and elevated inflammatory cytokine levels in the olfactory bulb. Additionally, we observed a down-regulation of Glu and an up-regulation of GABA in the synaptic gaps of the olfactory bulb, which contributed to a decreased discharge rate of M/Ts. Intervention with dexamethasone effectively reversed these changes and improved olfactory function. Our findings suggest that neuroinflammation within the olfactory bulb plays a significant role in the pathogenesis of olfactory dysfunction associated with chronic rhinosinusitis.

Acknowledgements

The authors are grateful to Prof. Lanqun Mao for his technical assistance.

Authorship contribution

ZZ conducted the experiments. FM and YZ gave technical support and conceptual advice. ZZ designed studies, interpreted the results, and wrote the article. FM and YZ made helpful revisions to the manuscript. All authors read and approved the final manuscript.

Conflict of interest

The authors declare no conflicts of interest in this work.

Funding

This research was supported by the National Natural Science Foundation of China (grant NO. 82271168).

References

- Shi JB, Fu QL, Zhang H, et al. Epidemiology of chronic rhinosinusitis: results from a cross-sectional survey in seven Chinese cities. Allergy. 2015. 70(5): 533-539.
- Hummel T, Whitcroft KL, Andrews P, et al. Position paper on olfactory dysfunction. Rhinol Suppl. 2017. 54(26): 1-30.
- Huang WH, Hung YW, Hung W, et al. Murine model of eosinophilic chronic rhinosinusitis with nasal polyposis inducing neuroinflammation and olfactory dysfunction. J Allergy Clin Immunol. 2024. 154(2): 325-339.
- 4. Raviv JR, Kern RC. Chronic sinusitis and olfactory dysfunction. Otolaryngol Clin North Am. 2004. 37(6): 1143-1157.
- 5. Shehata EM, Tomoum MO, Amer MA, et

- al. Olfactory bulb neuroplasticity: a prospective cohort study in patients with chronic rhinosinusitis with nasal polyps. Clin Otolaryngol. 2018. 43(6): 1528-1534.
- Doorn KJ, Goudriaan A, Blits-Huizinga C, et al. Increased amoeboid microglial density in the olfactory bulb of Parkinson's and Alzheimer's patients. Brain Pathol. 2014. 24(2): 152-165.
- Reale M, D'Angelo C, Costantini E, et al. Expression profiling of cytokine, cholinergic markers, and amyloid-β deposition in the APPSWE/PS1dE9 mouse model of Alzheimer's Disease pathology. J Alzheimers Dis. 2018. 62(1): 467-476.
- 8. LaFever BJ, Kawasawa YI, Ito A, et al. Pathological consequences of chronic

- olfactory inflammation on neurite morphology of olfactory bulb projection neurons. Brain Behav Immun Health. 2022. 21: 100451.
- Yeh CF, Huang WH, Lan MY, et al. Lipopolysaccharide-initiated rhinosinusitis causes neuroinflammation and olfactory dysfunction in mice. Am J Rhinol Allergy. 2023. 37(3): 298-306.
- Alobid I, Benítez P, Cardelús S, et al. Oral plus nasal corticosteroids improve smell, nasal congestion, and inflammation in sinonasal polyposis. Laryngoscope. 2014. 124(1): 50-56.
- Tanaka J, Fujita H, Matsuda S, et al. Glucocorticoid- and mineralocorticoid receptors in microglial cells: the two recep-

CRS-induced olfactory dysfunction and neuroinflammation

- tors mediate differential effects of corticosteroids. Glia. 1997. 20(1): 23-37.
- Kim HC, Lim JY, Kim S, et al. Development of a mouse model of eosinophilic chronic rhinosinusitis with nasal polyp by nasal instillation of an Aspergillus protease and ovalbumin. Eur Arch Otorhinolaryngol. 2017. 274(11): 3899-3906.
- Ohshima M, Taguchi A, Tsuda H, et al. Intraperitoneal and intravenous deliveries are not comparable in terms of drug efficacy and cell distribution in neonatal mice with hypoxia-ischemia. Brain Dev, 2015,37(4):376-386.
- 14. Yang M, Crawley JN. Simple behavioral assessment of mouse olfaction. Curr Protoc Neurosci. 2009. Chapter 8: Unit 8.24.
- 15. Paxinos G, Watson C. The rat brain stereotaxic coordinates. 2007.
- Xiong S, Song Y, Liu J, et al. Neuroprotective effects of MK-801 on auditory cortex in salicylate-induced tinnitus: Involvement of neural activity, glutamate and ascorbate. Hear Res. 2019. 375: 44-52.
- 17. Stephan H, Frahm HD, Baron G. Comparison of brain structure volumes in Insectivora and primates. VII. Amygdaloid components. J Hirnforsch. 1987. 28(5): 571-584.
- Rouyar A, Classe M, Gorski R, et al. Type 2/ Th2-driven inflammation impairs olfactory sensory neurogenesis in the mouse chronic rhinosinusitis model. Allergy. 2019. 74(3): 549-559
- Rothhammer V, Quintana FJ. Role of astrocytes and microglia in central nervous system inflammation. Introduction. Semin Immunopathol. 2015. 37(6): 575-576.
- Hasegawa-Ishii S, Shimada A, Imamura F. Neuroplastic changes in the olfactory bulb associated with nasal inflammation in mice.

- J Allergy Clin Immunol. 2019. 143(3): 978-
- 21. Kagoya R, Toma-Hirano M, Yamagishi J, et al. Immunological status of the olfactory bulb in a murine model of Toll-like receptor 3-mediated upper respiratory tract inflammation. J Neuroinflammation. 2022. 19(1): 13.
- Nagayama S, Homma R, Imamura F. Neuronal organization of olfactory bulb circuits. Front Neural Circuits. 2014. 8: 98.
- 23. Xu Z, Wang L, Chen G, et al. Roles of GSK3β in odor habituation and spontaneous neural activity of the mouse olfactory bulb. PLoS One. 2013. 8(5): e63598.
- 24. Zhao Y, Wang B, Gao Y, et al. Olfactory ensheathing cell apoptosis induced by hypoxia and serum deprivation. Neurosci Lett. 2007. 421(3): 197-202.
- Hernández-Soto R, Villasana-Salazar B, Pinedo-Vargas L, et al. Chronic intermittent hypoxia alters main olfactory bulb activity and olfaction. Exp Neurol. 2021. 340: 113653.
- Ahnaou A, Rodriguez-Manrique D, Embrechts S, et al. Aging alters olfactory bulb network oscillations and connectivity: relevance for aging-related neurodegeneration studies. Neural Plast. 2020. 2020: 1703969.
- Glass CK, Saijo K, Winner B, et al. Mechanisms underlying inflammation in neurodegeneration. Cell. 2010. 140(6): 918-34
- 28. Kwon HS, Koh SH. Neuroinflammation in neurodegenerative disorders: the roles of microglia and astrocytes. Transl Neurodegener. 2020. 9(1): 42.
- 29. Whitehouse MW. Anti-inflammatory gluco-corticoid drugs: reflections after 60 years.

- Inflammopharmacology. 2011. 19(1): 1-19.
- Hinkerohe D, Smikalla D, Schoebel A, et al. Dexamethasone prevents LPS-induced microglial activation and astroglial impairment in an experimental bacterial meningitis co-culture model. Brain Res. 2010. 1329: 45-54.
- 31. Soltani A, Chugaeva UY, Ramadan MF, et al. A narrative review of the effects of dexamethasone on traumatic brain injury in clinical and animal studies: focusing on inflammation. Inflammopharmacology. 2023. 31(6): 2955-2971.
- Chantong B, Kratschmar DV, Nashev LG, et al. Mineralocorticoid and glucocorticoid receptors differentially regulate NF-kappaB activity and pro-inflammatory cytokine production in murine BV-2 microglial cells. J Neuroinflammation. 2012. 9: 260.
- Meneses G, Gevorkian G, Florentino A, et al. Intranasal delivery of dexamethasone efficiently controls LPS-induced murine neuroinflammation. Clin Exp Immunol. 2017. 190(3): 304-314.

Yinghong Zhang and Furong Ma Department Otolaryngology Head and Neck Surgery Peking University Third Hospital Beijing 100191 China

* E-mails: yinghongzhang@bjmu.edu.cn furongma@126.com

Zhidi Zhang¹, Yali Du¹, Shan Xiong¹, Wanxin Cao², Hailing Jiang¹, Jiayue Wang¹, Mengqin Li¹, Ying Hu1, Furong Ma^{1*}, Yinghong Zhang^{1*}

 $^1\, {\sf Department}\ {\sf of}\ {\sf Otolaryngology-Head}\ {\sf and}\ {\sf Neck}\ {\sf Surgery}, {\sf Peking}\ {\sf University}\ {\sf Third}\ {\sf Hospital}, {\sf Beijing}, {\sf China}\ {$

 $^2\, Department \ of \ Otolaryngology, Ren \ Ji \ Hospital, Shanghai \ Jiao \ Tong \ University \ School \ of \ Medicine, Shanghai, China$

Rhinology 64: 1, 0 - 0, 2026 https://doi.org/10.4193/Rhin25.164

Received for publication:

March 26, 2025

Accepted: Auguts 6, 2025

Associate Editor:

Basile Landis

Zhang et al.

SUPPLEMENTARY MATERIAL

Supplementary Method 1

CRS-OD group: sensitized experimental rats were injected intraperitoneally with 2 mg of aluminum hydroxide solution mixed with 125ug OVA on day 0 and day 4 of week 1.525ug OVA diluted in 210 uL of sterile phosphate-buffered saline (PBS) was injected into the nasal cavities of the rats by drip injection for 5 consecutive days in week 2. A mixture of 525 µg of OVA and 3.78 U of Aspergillus oryzae protease (Sigma) was added to the PBS solution and diluted to 210 µl, and the rats were injected nasally three times a week from week 3 to week 8. Control group: SD rats were given PBS solution at the same time point. Saline group: rats in the experimental group were given an equal dose of saline intraperitoneally for 7 consecutive days starting at week 9. Dexamethasone group (Dex group): rats in the experimental group were given intraperitoneal injections of dexamethasone at 2 mg/kg starting at week 9 for 7 consecutive days.

Supplementary Method 2

Clean bedding was evenly spread on a clean laboratory rat cage ($45 \text{ cm} \times 24 \text{ cm} \times 20 \text{ cm}$) with a thickness of about 3 cm, and 1 piece of rat food (1 cm \times 1 cm \times 1 cm) was buried under the bedding as bait for about 0.5 cm, so that the rat food was completely buried until it was out of sight. The rats were fasted for 24 hours before the test and placed in the cage for 10 minutes. The rats were placed in the center of the cage and a timer was pressed to start the timer. When the rats found the food and started to eat, the timer was pressed to stop the timer, and the time was recorded as the time the rats spent searching for the food. If the rat does not find the food within 360 seconds, the timer will be stopped and the time of 360 seconds will be recorded. Each rat was tested 3 times at 1-hour intervals, and the final average of the rats' search time was taken.

Supplementary Method 3

In 4µm paraffin sections of tissues, high-pressure repair was performed after deparaffinization, endogenous peroxidase was blocked, serum was blocked at room temperature, primary antibody was added overnight, goat anti-mouse IgG (K5007, DAKO) was added dropwise, DAB was used to develop the color, and the nuclei of the cells were stained with hematoxylin, and the slices were sealed by dehydration. Immunohistochemical analysis was performed under a microscope.

Supplementary Method 4

Paraffin sections were deparaffinized to water, antigenically repaired, and closed at room temperature. Next, the sections were incubated with anti-Iba-1 antibody (ab178846, Abcam) at 4 °C overnight. On the following day, the samples were incubated with the primary antibody of the corresponding species for 1 h. The samples were washed with PBS and stained with 4',6-diamidino-2-phenylindole (DAPI). The film was sealed with an autofluorescence quenching sealer and observed under a fluorescence microscope.